Industrial Crops & Products 225 (2025) 120464

Contents lists available at ScienceDirect

Industrial Crops & Products

journal homepage: www.elsevier.com/locate/indcrop

Synergistic effects of aged lignin-based biochar and selenium fertilization on heavy metal remediation in agricultural soils

Xianzhen Li [a], Yongchao Yu [a], Ruimei He [a], Qing Zhen [b,c,*], Diao She [b,c,*]

[a] College of Natural Resources and Environment, Northwest A&F University, Yangling, Shaanxi 712100, China
[b] College of Soil and Water Conservation Science and Engineering, Northwest A&F University, Yangling, Shaanxi 712100, China
[c] Institute of Soil and Water Conservation, Chinese Academy of Sciences and Ministry of Water Resource, Yangling, Shaanxi 712100, China

ARTICLE INFO

Keywords:
Lignin
Biochar
Selenium
Adsorption
Heavy metal
Remediation

ABSTRACT

The widespread contamination of soils with heavy metals, such as cadmium (Cd) and zinc (Zn), presents significant threats to agricultural productivity and environmental health. Biochar (BC) and selenium (Se) have significant potential to alleviate soil heavy metal contamination and ensure crop safety. However, the current understanding of the property changes in aged lignin-based biochar and its interaction with Se in enhancing plant resistance remains limited. This study investigates the potential of aged lignin-based biochar (LBC) and foliar-applied selenium (Se) to mitigate heavy metal contamination and enhance *pakchoi* growth in soils contaminated with cadmium (Cd) and zinc (Zn). Results indicate that aging of LBC facilitated the formation of C–O and Si–O groups, with mineral components transitioning from MgO and Mg_2SiO_4 to stable forms of SiO_2 and Ca, $MgCO_3$. Additionally, during the adsorption of Cd^{2+} and Zn^{2+}, the contribution of minerals decreased, while that of non-mineral components increased, with a shift from the Freundlich to the Langmuir adsorption model. Furthermore, the synergistic effect of aged LBC with foliar Se significantly enhanced *pakchoi*'s photosynthesis and antioxidant enzyme activity of *pakchoi*, isolatied Cd^{2+} and Zn^{2+} in vacuoles and cell walls, and effectively reduced the uptake of these metals and mitigating their toxicity. This research offers novel insights into the synergistic effects of aged LBC and Se on heavy metal remediation in agricultural soils, offering a sustainable strategy to improving food safety and soil health.

1. Introduction

Soil contamination with heavy metals is a critical global issue that jeopardizes agricultural productivity and environmental health (Tóth et al., 2016). Pollutants such as cadmium (Cd) and zinc (Zn) are pervasive, with their impact intensifying due to industrial activities like mining, smelting, and the extensive use of fertilizers (Roberts, 2014). High concentrations of Cd and Zn pollution negatively impact soil biodiversity and quality (Bandara et al., 2019), disrupt plant physiology, and may harm human organs, including the kidneys and reproductive system, through the food chain (Hou et al., 2022; Meng et al., 2024).

Leafy vegetables are particularly prone to absorbing cadmium and zinc from contaminated soils, thereby acting as vectors for these heavy metals in the human diet and exacerbating public health risks (Ouyang et al., 2022). This underscores the urgent need for effective soil remediation strategies to mitigate the toxicity of heavy metals. Biochar (BC), a high-carbon material produced via the pyrolysis of biomass, has garnered attention for its potential in heavy metal pollution control and soil remediation (Bolan et al., 2023). Lignin-derived biochar (LB) offers enhanced structural stability and nutrient retention due to its aromatic polymer structure, which reduces degradation under environmental stresses (Yuan et al., 2021). Its high surface area and abundance of functional groups improve soil properties and microbial activity, thereby promoting plant growth (Bolan et al., 2021). Furthermore, the modification of LB with minerals such as silicon and magnesium significantly enhance its ability to immobilize heavy metals and improve soil fertility (Menzembere et al., 2023; Li et al., 2024a).

These modifications introduce functional groups (O=C–O, Si–O, Mg–O) on the LB surface, which increase its structural stability and reduce the availability of Cd and Zn in the soil (Li et al., 2024a), positioning LB as a promising material for sustainable soil management and ecological restoration.

Recent efforts to combat heavy metal soil pollution have focused on reducing plant uptake of these metals. Studies show that LBC, combined

* Corresponding authors at: College of Soil and Water Conservation Science and Engineering, Northwest A&F University, Yangling, Shaanxi 712100, China.
E-mail addresses: zhenqing10@nwafu.edu.cn (Q. Zhen), diaoshe@ms.iswc.ac.cn (D. She).

https://doi.org/10.1016/j.indcrop.2025.120464
Received 30 September 2024; Received in revised form 25 December 2024; Accepted 1 January 2025
Available online 11 January 2025

with foliar Se fertilizer application, effectively mitigates heavy metal toxicity in vegetables, boosts antioxidant capacity, and reduces metal uptake (Li et al., 2024b). While this combination demonstrates significant initial remediation effects, further research on the aging of biochar and its interactions with foliar Se over time is necessary to optimize long-term remediation outcomes.

Lignin content plays a vital role in enhancing the properties of BC, particularly its thermal stability and interactions with soil components (Bolan et al., 2021). The complex aromatic structure of lignin improves BC's ability to withstand environmental stresses and maintain its integrity over extended periods, making it well-suited for long-term soil remediation (Kim et al., 2024). Additionally, LB features a high density of functional groups, such as hydroxyl (–OH) and carboxyl (–COOH), which facilitate the adsorption of heavy metals through chemical bonding, thereby improving its effectiveness in contaminated soil remediation (Yuan et al., 2021). Moreover, LBC interacts positively with soil minerals, releasing essential nutrients like magnesium and silicon that promote plant growth and microbial diversity, thus enhancing its ecological benefits (Bandara et al., 2022). However, despite its greater stability and heavy metal remediation capabilities compared to other biomass-based BCs, LB undergoes aging processes in soil such as mechanical fragmentation, surface oxidation and mineral dissolution, thereby altering its structure and function (Shen et al., 2024; Chen et al., 2024; Mia et al., 2018). Aging may lead to nutrient and mineral depletion, reducing its capacity for heavy metal immobilization and adsorption (Lehmann, 2007; Meng et al., 2024), while increasing its polarity and hydrophilicity, which facilitates organic compound formation and alters soil chemical and biological properties (Marcińczyk et al., 2024; Krzyszczak et al., 2022). Thus, understanding the mechanisms of LBC aging and its post-aging synergistic effects is essential for optimizing its long-term remediation potential.

This study investigates the potential of LBC combined with aging treatment in heavy metal removal and plant growth improvement, with a focus on its interaction with Se. Unlike previous studies, this research reveals the long-term effects of the LBC aging process and Se on plant growth promotion, while clarifying the stability and effectiveness of lignin-derived biochar during prolonged use. This study focuses on: 1) the dynamic changes in the surface structure of LBC following the aging process; 2) the characteristic changes and mechanisms of LBC in the adsorption of Cd^{2+} and Zn^{2+} post-aging; and 3) the synergistic mechanisms of aging LBC combined with foliar application of Se fertilizer in remediating soils contaminated with heavy metals (Cd^{2+} and Zn^{2+}). These findings provide a theoretical foundation for enhancing our understanding of LBC applications and establish a solid scientific basis for developing sustainable strategies to manage heavy metal-contaminated soils, advancing green agriculture and food safety.

2. Materials and methods

2.1. Preparation of materials and soil properties

Using abundant lignin from paper waste as a raw material for preparing LBC is a green and sustainable approach to resource utilization. The lignin used in this study was sourced from Shandong Longli Company. Industrial lignin and sodium silicate were dissolved in 100 mL of deionized water at a ratio of 1:1, and the pH of the solution was adjusted with HCl. Subsequently, the mixed solution was then placed in a hydrothermal reaction kettle and subjected to a reaction at 160°C for 2 h. Following the reaction, the solid product was immersed in a 1 M $MgCl_2$ solution for treatment. The immersed samples were dried to remove residual moisture and then subjected to high–temperature treatment at 500°C under anaerobic conditions for 2 h. Finally, the samples were rinsed with deionized water to neutralize and obtain the desired LBC samples. For evaluating the application effectiveness of LBC in soil, farmland soil from Fengxian County, Baoji City, Shaanxi Province, China (35°28′N, 104°44′E), was selected as the experimental soil. The soil sample is representative, contaminated with Cd and Zn, and reflects the common characteristics of polluted farmland soil in the area. The fundamental properties of the soil are outlined in Table S1. Schematic representation of the experimental workflow is in Fig. S1.

2.2. Simulated aging and pot experiment design

The chemical stability of LBC may be more susceptible to aging processes, with factors influencing its anti–aging ability in soil primarily encompassing rainfall and temperature variations (Meng et al., 2022). Based on meteorological data from Baoji City, this study simulated the aging process of LBC in soil, including wet–dry and freeze–thaw cycles. To collect aged LBC for studying the changes in its physicochemical properties and its effectiveness in passivating Cd and Zn. A 1 % modified LBC teabag test was conducted by burying it in culture bottles with contaminated soil, saturating the soil with deionized water, incubating at a constant temperature (25°C) for 24 h, followed by drying at 40°C for 24 h; this process was repeated five times to complete the wet–dry cycle. Subsequently, the moisture content of the soil with added LBC was maintained at 20 %, incubated in a constant temperature incubator (25°C) for 24 h, and then frozen for 12 h at –12°C; this process was repeated three times. These cycles constitute a simulation of one year of natural aging. This study performed three combined aging cycles, simulating three years of natural aging, with samples from the first, second, and third years labeled as LBC1, LBC2, and LBC3, respectively. A control treatment was conducted under constant temperature and humidity conditions, labeled as LBC0. After the aging incubation, the teabags containing LBC were removed to study the changes in the LBC and its passivation capabilities. LBC was added to 2 kg of soil at a 1 % incorporation rate and mixed evenly. The aging of the potted soil was the same as the treatment described above; after the simulated aging process, the soil was air–dried, sifted, and repotted for the pot experiment. This study found that constant temperature and humidity aging had a minimal effect on LBC, so the pot experiment design included: original soil (CK), soils with LBC aged for 1, 2, and 3 years ($Soil_{LBC1}$, $Soil_{LBC2}$, $Soil_{LBC3}$), original soil with foliar Se fertilizer (CK+Se), and soils with LBC and foliar Se fertilizer aged for 1, 2, and 3 years ($Soil_{LBC1}$+Se, $Soil_{LBC2}$+Se, $Soil_{LBC3}$+Se), totaling eight treatments, with three replicates each. Foliar Se fertilizer was sprayed at 4 PM, once a week, for a total of four applications. For treatments without foliar Se fertilizer, deionized water was used instead, and the top of the pots was covered with tin foil during spraying to prevent Se fertilizer from entering the soil.

2.3. Characteristics and mechanisms of Cd^{2+} and Zn^{2+} adsorption by aged LBC in a mixed Cd^{2+} and Zn^{2+} system

The characteristics of isothermal adsorption and time–dependent adsorption of Cd^{2+} and Zn^{2+} by aged LBC were investigated in the Cd and Zn system. Solutions of Cd^{2+} and Zn^{2+} at 1000 mg/L were prepared using $Cd(NO_3)_2$ and $Zn(NO_3)_2$, and then diluted to the desired concentrations. An adsorption test was conducted by adding 0.02 g of aged LBC to 50 mL of Cd^{2+} and Zn^{2+} solution in a 100 mL centrifuge tube, shaken at 200 rpm for 24 h in a constant temperature shaker to explore the adsorption characteristics of Cd^{2+} and Zn^{2+} at concentrations (20–200 mg/L) over time (0–480 min). The mixture was filtered through a 0.45 μm filter, and the filtrate concentrations were measured by atomic absorption. The aged LBC was demineralized by soaking in 1 M HCl, shaken at 220 rpm for 24 h, then the LBC was collected and dried for subsequent adsorption tests. The adsorption capacity for Cd and Zn after demineralization was contributed by the non–mineral portion of the LBC. The difference in adsorption capacity for Cd and Zn between aged and demineralized LBC represents the contribution from the mineral portion. All experiments were conducted in triplicate, and the results presented are averages. The formula used is described in Table S2. Detailed characterization of the aged LBC samples can be found in Text

S1.

2.4. Determination of the biomass, chlorophyll content and photosynthetic parameters of pakchoi

Before harvesting, gas exchange parameters, including stomatal conductance (G_s), net photosynthetic rate (P_n), and transpiration rate (T_r), were recorded using the American Hansatech CIRAS–3 portable photosynthesis system. Three leaves were selected for measurement, and three repeated measurements were taken at each leaf position to calculate the average value. After harvesting, the plants were immediately weighed using a balance, and their fresh weight data were recorded. Subsequently, these fresh plant samples were oven–dried until a constant weight was reached to obtain plant dry weight data. 3–4 tender leaves closest to the root of each plant were collected, washed, and dried with distilled water, then quickly frozen in liquid nitrogen. The relative chlorophyll content in the leaves was extracted with 95 % ethanol and subsequently quantified by absorbance measurements at 665 nm, 649 nm, and 470 nm (Arnon, 1949).

2.5. Determination of the antioxidant indices and subcellular distribution

The activity of SOD was extracted from phosphate buffer (7.8 pH) homogenate, and the supernatant was obtained after centrifugation and determined by nitrogen blue tetrazolium-photo-reduction method (Fridovich, 1975). CAT activity was extracted from phosphate buffer (7.8 pH) homogenate, and the supernatant was taken after centrifugation to measure the catalase activity according to the rate of absorbance change (Aebi, 1984). GSH was extracted with 5 % metaphosphoric acid homogenate. After centrifugation, the supernatant was obtained and its concentration was determined with DTNB for color development at 412 nm (Noctor and Foyer, 1998). MDA was extracted from TCA homogenates. After centrifugation, thiobarbituric acid method was used to estimate MDA of leaves (Heath and Packer, 1968). The Cd and Zn subcellular distribution were determined according to the method described by Huang et al., (2021) with some appropriate modifications. The specific method was described in detail in the supplementary materials (Text S2).

2.6. Si, Mg, Cd and Zn content measurements and Cd and Zn translocation factors calculation

Exchangeable magnesium was extracted from soil using ammonium acetate, and its measurement was conducted using Flame Atomic Absorption Spectrometer AAS (PE 900 T). Available silicon in soil was extracted using citric acid, and analysis was performed using the silicomolybdenum blue colorimetric method. Heavy metal forms in soil were assessed by microwave digestion with a mixed acid solution (including HCl, HNO_3, $HClO_4$, and HF), followed by measurement. The forms of heavy metals in soil were primarily classified into exchangeable (F1), carbonate–bound (F2), Fe–Mn oxide–bound (F3), organic–bound (F4), and residual (F5), with detailed procedures provided in Table S3. For the elements Cd, Zn, Si, and Mg in vegetable tissues, digestion was performed with a mixed acid solution, followed by measurement using Flame Atomic Absorption Spectrometer AAS (PE 900 T). Silicon content in the vegetable tissues was determined using the silicomolybdenum blue colorimetric method and expressed based on plant dry weight.

3. Results and discussion

3.1. Physicochemical changes in aged LBC

Aging significantly altered the surface morphology of biochar. In LBC0 samples, the carbon pore walls appeared rough, whereas in LBC3, particles coalesced into a contiguous form, indicating structural changes (Fig. 1). Functional group analysis revealed minor but notable shifts in intensity and positions of key functional groups, such as O–H stretching vibrations (3489–3226 cm^{-1}), C═C skeletal vibrations

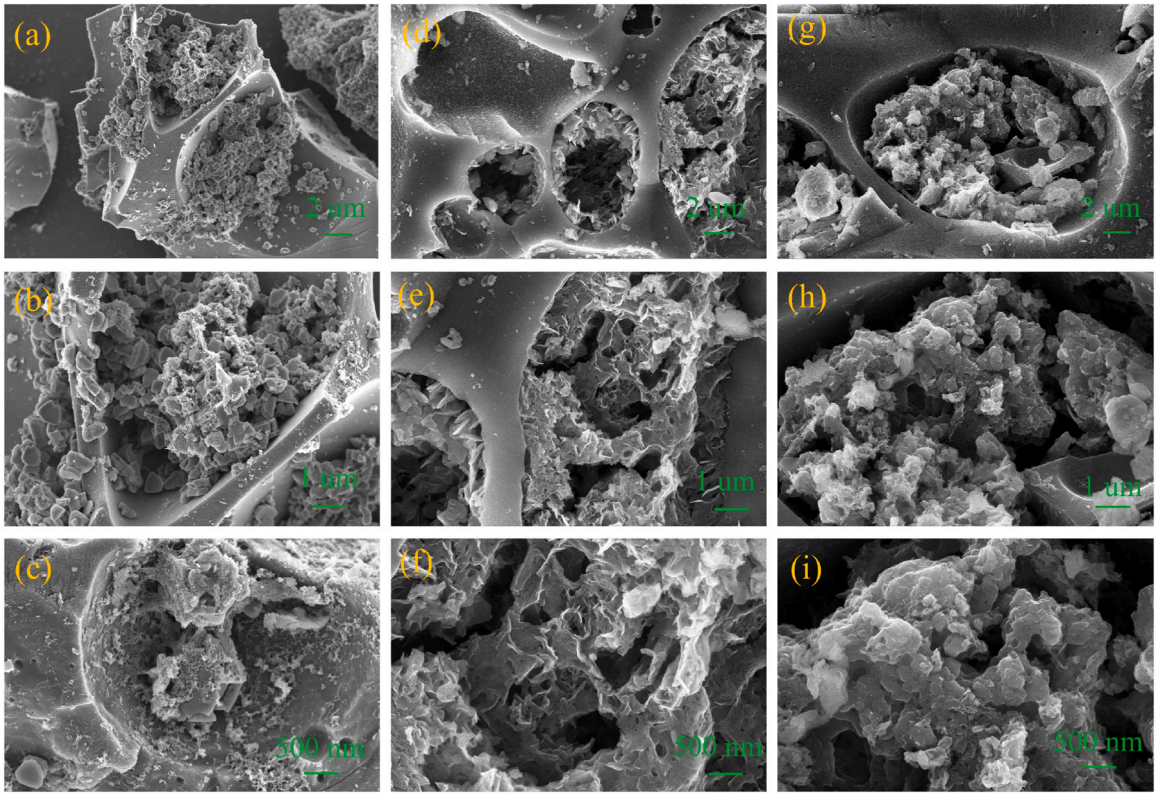

Fig. 1. SEM images of OLBC(a, *b*, c), LBC0(d, e, f), and LBC3(g, h, i).

(1598–1556 cm^{-1}), C–H bending vibrations (1445–1363 cm^{-1}), Si–O (1000 cm^{-1}), and Mg–O (869–619 cm^{-1}). These changes suggest enhanced chemical reactivity and adsorption potential due to aging (Fig. 2a). Notably, the mineral components in the LBC changed significantly from initially being dominated by MgO (PDF#89–4248) and Mg_2SiO_4 (PDF#84–1402), to primarily $CaCO_3$ (PDF#76–0606), Ca, $MgCO_3$ (PDF#43–0697), and SiO_2 (PDF#79–1906) after aging (Fig. 2c). This indicates that Mg–containing minerals were gradually replaced by Ca–containing minerals during aging, which could potentially affect the adsorptive properties of the LBC.

XPS results (Fig. 2d–g) showed a decreased C1s peak intensity and an increased O1s peak intensity, attributable to the decomposition of unstable carbon components on the LBC surface during aging, which facilitated the formation of oxygen–containing groups. The high–resolution C1s spectrum reveals that the C–C peak areas for OLBC, LBC0, and LBC3 are 72.96 %, 65.25 %, and 61.51 % respectively, with increasing areas for C–O and C–C═O peaks, indicative of C–C bond consumption and the formation of C–O and C═O groups during aging. An enlarged C═O peak area in the O1s high–resolution spectrum corroborates this conclusion. The C1s and O1s peak areas for BC suggest significant alterations due to simulated aging. Si 2p analysis reveals an increase in Si–O peak areas for LBC0 and LBC3 relative to OLBC, especially in LBC3 where the C–Si peak area is notably smaller. This indicates that aging promotes the formation of Si–O groups while consuming C–Si groups. Mg1s analysis indicates that aging results in a decrease in MgO peak area and an increase in Mg–X peak area, reflecting the consumption of MgO and the proliferation of Mg–X.

3.2. Cd and Zn adsorption characteristics and mechanisms by aging LBC

In a mixed Cd and Zn system, LBC showed variable adsorption behaviors over different aging periods (Fig. 3a–h). Overall, LBC's adsorption capacity was significantly higher for Zn than for Cd, decreasing gradually for both metals as the aging period progressed. This trend could be attributed to mineral composition changes during aging, particularly the formation of stable minerals like $CaCO_3$ and Ca, $MgCO_3$. Compared to the original MgO and Na_2SiO_4, these newly formed minerals possess lower cation exchange capacities, thereby reducing the LBC's efficiency in adsorbing heavy metal ions. Additionally, the formation of SiO_2 limited the role of silica–containing minerals in ion exchange and mineral precipitation processes.

Adsorption data fitted using the Langmuir and Freundlich models (Tables S4 and Fig. 3) demonstrated that under normal and single aging conditions, the Freundlich model yielded higher R^2 values and lower Δq values. This suggests that LBC adsorption of Cd and Zn likely relies more on chemisorption, predominantly occurring on heterogeneous surfaces. However, after two aging cycles, the adsorption characteristics of LBC2 and LBC3 for Cd and Zn changed, with the R^2 values for the Langmuir model surpassing those of the Freundlich model. This transition from heterogeneous to homogeneous surface adsorption indicates that chemisorption became the dominant mechanism during aging, supported by the formation of stable functional groups (Si–O and C–O) and mineral components (Ca,$MgCO_3$). Kinetic simulations (Fig. 3e–h and Table S5) show that aged LBC rapidly adsorbs Cd and Zn within the first 120 minutes. This rapid adsorption is attributed to numerous adsorption sites on the LBC surface and a significant concentration gradient between the liquid and solid phases. Notably, the adsorption rate and

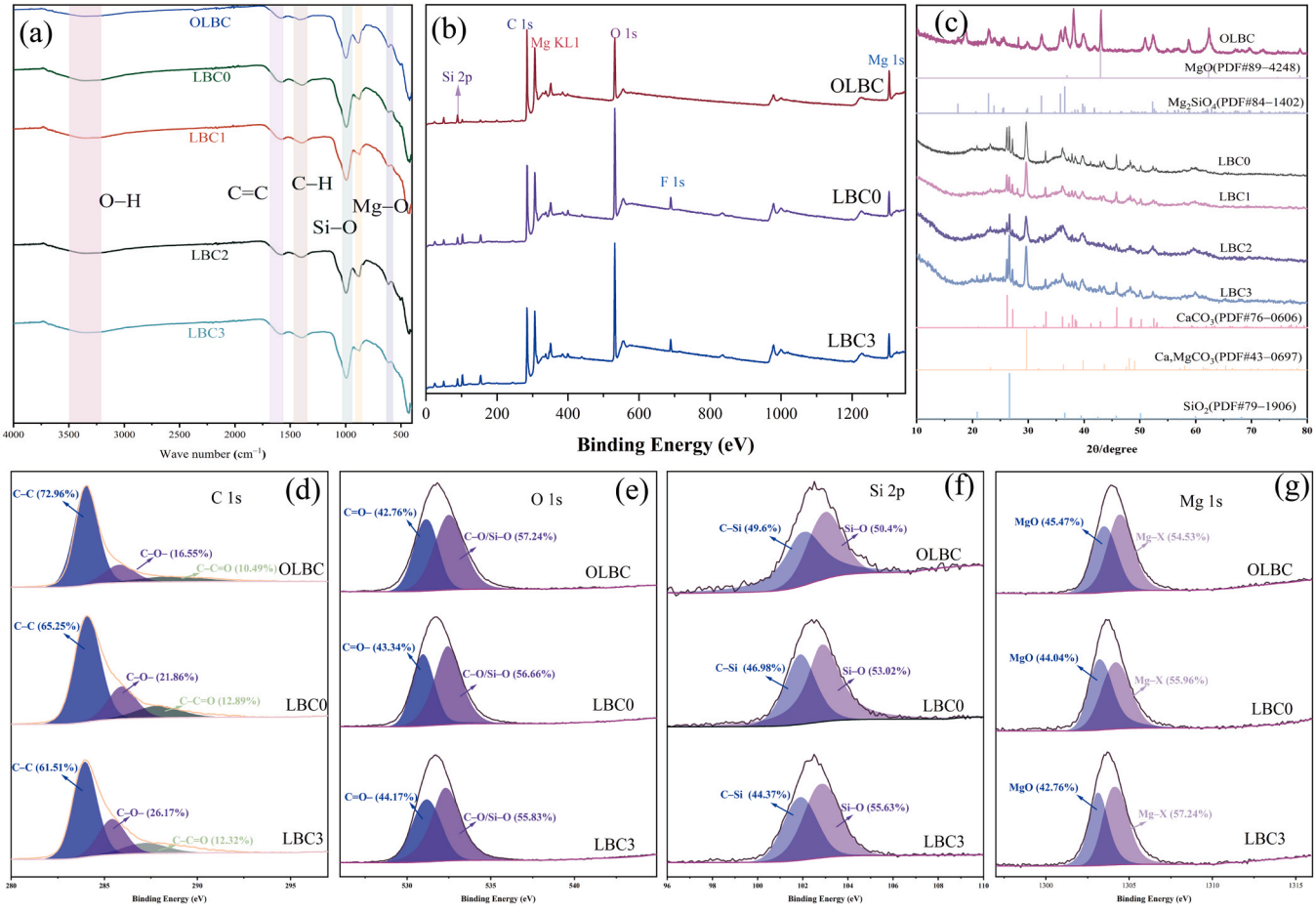

Fig. 2. FTIR (a), XPS (b), XRD (c), C 1 s (d), O 1 s (e), Si 2p (f), and Mg 1 s (g) spectra of OLBC, LBC0 and LBC3.

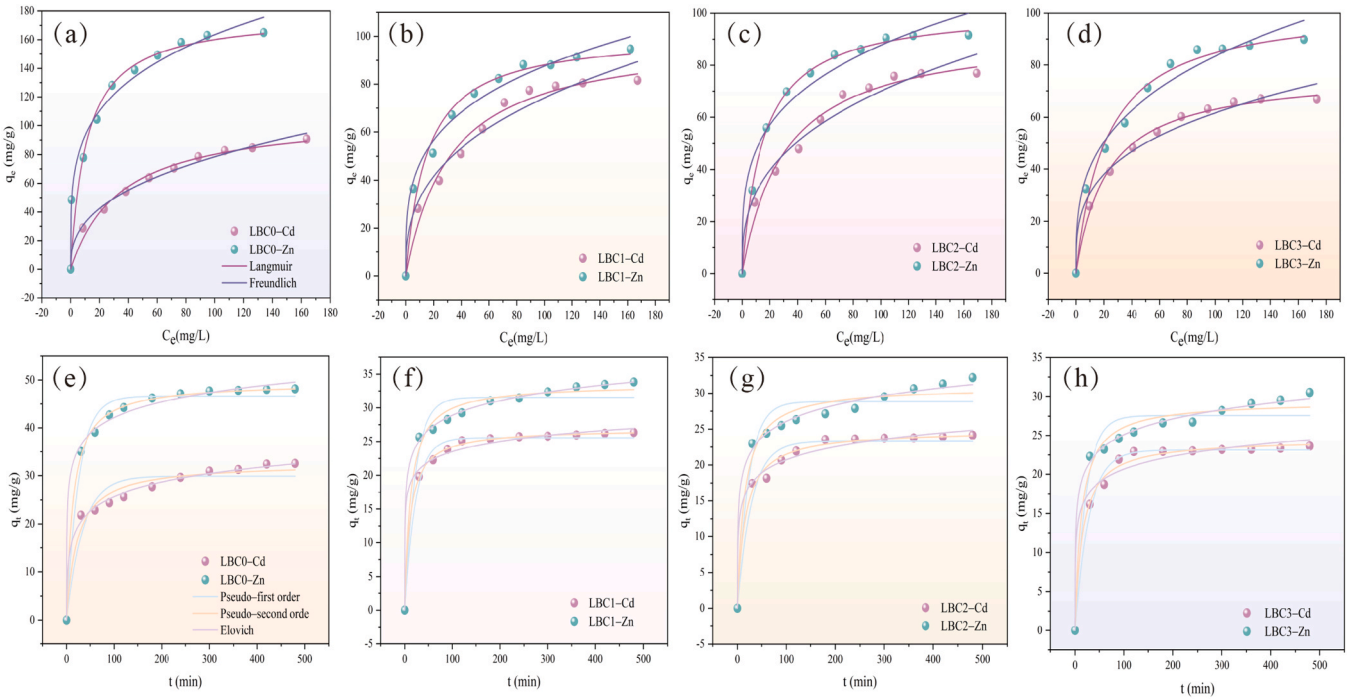

Fig. 3. Adsorption isotherms (a-d) and adsorption kinetics (e-h) data and fitted models of Cd^{2+}, and Zn^{2+} onto LBC0, LBC1, LBC2, and LBC3.

capacity of LBC for Zn^{2+} are superior to that for Cd^{2+}, which may be related to Zn's higher electronegativity and larger hydration radius. High R^2 values and low Δq values from the pseudo–second–order kinetics and Elovich models indicate that adsorption of Cd and Zn by aged LBC in the system is predominantly driven by chemical processes.

LBC0 and LBC3 demonstrate distinct adsorption mechanisms for Cd and Zn within a mixed system. Characterizations of these LBCs, before and after adsorption, are shown in Figs. 2 and 4. After aging, the types of surface functional groups on LBC0 and LBC3 remained largely unchanged (Fig. 2a). After adsorbing Cd and Zn, significant changes occurred in FTIR spectrum of LBC at 1000 and 890 cm^{-1}, corresponding to Si–O and Mg–O, respectively, while other characteristic peak intensities and positions changed only slightly (Fig. 4a). All characteristic peak intensities and positions in LBC3 underwent slight changes as well. XRD spectra (Fig. 4b, c) indicate that after LBC adsorbed Cd and Zn, $CaCO_3$ may have been consumed through ion exchange and mineral precipitation, with the main mineral components changing to $Ca,MgCO_3$ (PDF#43–0697) and SiO_2 (PDF#79–1906). After adsorbing Cd and Zn, SiO_2 was not detected in LBC3. Following Cd and Zn adsorption, SiO_2 was undetected in LBC3, with $Ca,MgCO_3$ emerging as the dominant mineral component, which is more stable and contributes less to adsorption capacity of LBC. With the increase of aging degree, the adsorption contributions of mineral components to Cd and Zn gradually decreased, while the adsorption contributions of non–mineral components gradually increased in the mixed system of Cd and Zn (Fig. S2). XPS analysis revealed characteristic peaks of Zn 2p and Cd 3d post–adsorption in LBC0 and LBC3, with a stronger Zn 2p peak in LBC0, indicative of a higher Zn adsorption capacity. Following Cd and Zn adsorption, C1s spectrum of LBC0 showed a reduction in C–O– and C–C═O peak areas from 21.86 % and 12.89–21.43 % and 8.73 %, respectively. In LBC3, these areas decreased from 26.17 % and 12.32–22.54 % and 7.46 %, respectively. In LBC3, more C–O– groups participated in the adsorption process, possibly due to an increase in oxygen–containing groups during aging. Si 2p peak analysis indicated a decrease in Si–O peak areas and an increase in C–Si peak areas following Cd and Zn adsorption by LBC0 and LBC3. Mg 1 s peak analysis showed a reduction in MgO peak area and an enhancement in Mg–X peak area. This suggests that during the adsorption of Cd and Zn, LBC0 and LBC3 consumed Si–O and MgO, with these components possibly existing on the char surface as C–Si and Mg–metal complexes. Cd 3d and Zn 2p peak analysis shows that in LBC0 and LBC3, Cd predominantly exists as Cd 3d3/2 and Cd 3d5/2, while Zn forms are primarily Zn 2p3/2 and Zn 2p1/2. Although peak areas vary, the proportions of Cd 3d3/2 and Zn 2p3/2 in both LBC0 and LBC3 exceed 60 %.

3.3. Soil property improvements and Cd/Zn bioavailability reduction

Biochar aging significantly alters soil ecosystems by releasing beneficial nutrients and improving soil structure. Treatment with aged LBC significantly altered soil properties such as pH, A–Si, EC, and E–Mg (Fig. 5). As aging time increased, the levels of A–Si, EC, and E–Mg in the soil increased significantly. The observed increase in available silicon (190.80 %) and exchangeable magnesium (730.34 %) indicates that aged LBC acts as a slow-release source of these essential elements, enhancing soil fertility over time (Chen et al., 2024; Lebrun et al., 2023). This nutrient release supports microbial activity, which plays a critical role in transforming soil organic matter and stabilizing heavy metals through microbial precipitation and adsorption processes (Bandara et al., 2022). Furthermore, previous studies demonstrated that the nutrient release from biochar over time enhances soil pH, which reduces the solubility of heavy metals and promotes their conversion into less bioavailable forms (Afzal et al., 2024; Menzembere et al., 2023). These ecosystem-wide benefits highlight the long-term advantages of biochar aging for sustainable soil management.

Under CK treatment, the distribution ratio of Cd forms in the soil was: F1 > F5 > F3 > F2 > F4. After three years of simulated aging, the distribution ratio of Cd forms in the soil changed to: F3 > F1 > F5 > F2 > F4. The proportions of F1 and F2 components decreased by 47.27 % and 31.11 %, respectively, while the proportions of F3, F4, and F5 increased by 118.97 %, 29.61 %, and 9.50 %, respectively. Under CK treatment, the distribution ratio of Zn forms in the soil was: F4 > F3 > F5 > F2 > F1. After three years of simulated aging, the order of Zn forms distribution in the soil did not change, but the proportions of F1 and F2 components decreased by 85.53 % and 91.32 %, respectively. Meanwhile, F3, F4, and F5 components increased by 14.05 %, 12.89 %, and 2.98 %, respectively. In CK–treated soils, Cd

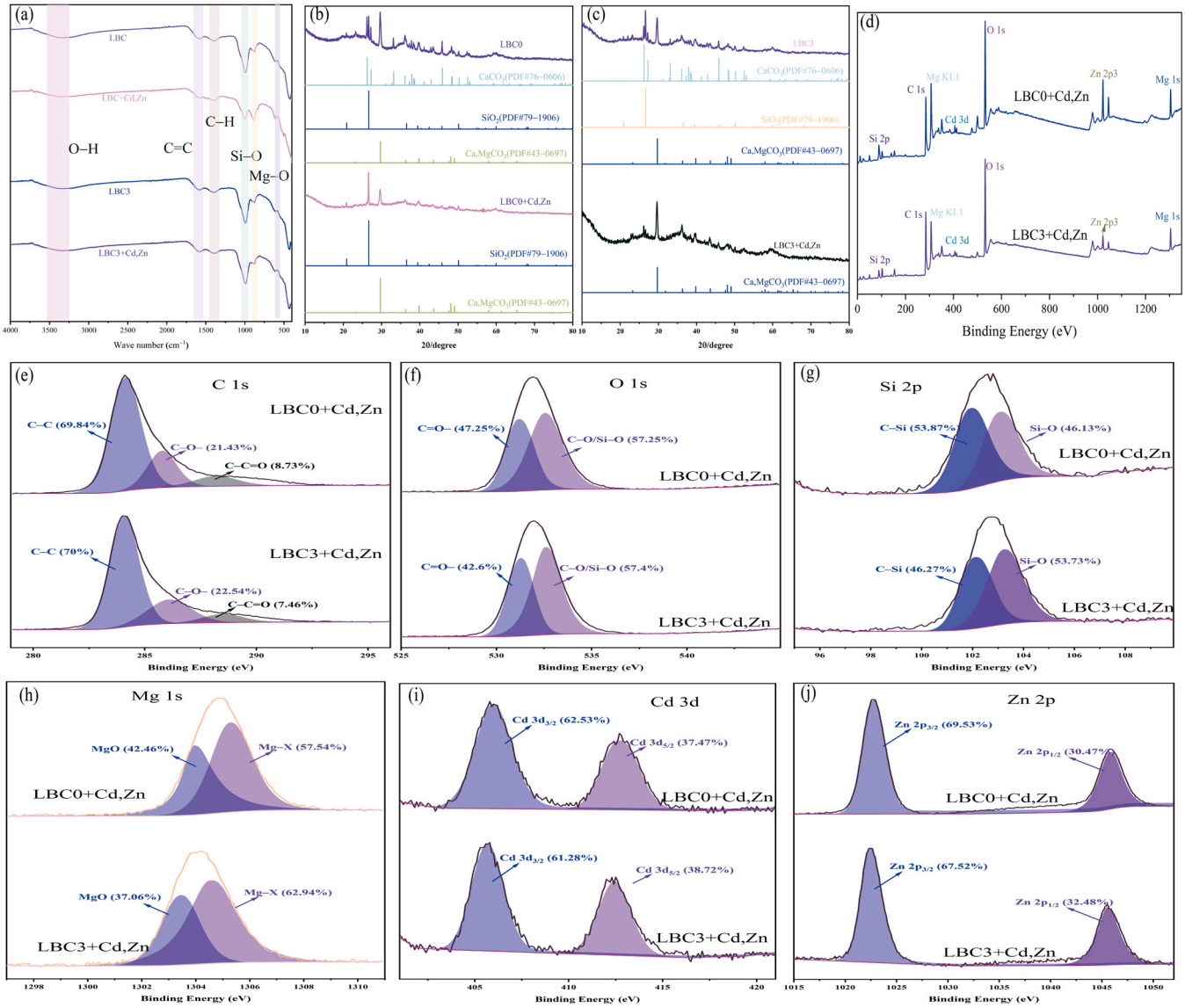

Fig. 4. The FTIR spectra (a), XRD spectra (b, c), XPS spectra (d) of LBC0 +Cd, Zn and LBC3 +Cd, Zn, C 1 s (e), O 1 s (f), Si 2p (g), Mg 1 s (h), Cd 3d (i), and Zn 2p (j) spectra of LBC0 +Cd, Zn and LBC3 +Cd, Zn.

and Zn mainly existed in highly mobile forms, increasing the risk of migration to plants and groundwater. After aging treatment, the proportion of mobile forms of Cd and Zn decreased significantly, while the proportion of more stable forms increased significantly. The reduction in heavy metal bioavailability observed in this study can be attributed to multiple mechanisms enhanced by LBC aging, including precipitation, complexation, and electrostatic adsorption. Aging promotes the formation of stable functional groups, such as C-O and Si-O, which increase the chemisorption capacity for Cd and Zn (Chen et al., 2024; Menzembere et al., 2023). The transition from Freundlich to Langmuir adsorption models further suggests that aged LBC provides more homogeneous adsorption sites, facilitating stronger chemical interactions with metal ions. Moreover, the formation of stable minerals like $Ca,MgCO_3$ and SiO_2 during aging adds to the immobilization of heavy metals via ion exchange and mineral precipitation (Bandara et al., 2022; Yuan et al., 2021). These findings align with previous studies, confirming that biochar aging not only stabilizes its structure but also enhances its functionality in heavy metal remediation (Chen et al., 2024).

Changes in surface properties during LBC aging are key factors. Aging increases the number of oxygens–containing functional groups on the LBC surface and enhances surface negative charge density, providing more binding sites for heavy metal ions. Meanwhile, given that Cd and Zn exhibit heightened mobility and bioavailability in acidic soils, increased soil pH promotes heavy metal precipitation, reducing their soluble and exchangeable forms (Khan et al., 2018). Furthermore, XRD spectra and exchangeable magnesium content data indicate that silicates and magnesium minerals in modified LBC undergo significant ion exchange with heavy metal ions in the soil during aging, promoting heavy metal immobilization.

To gain a deeper understanding of the effectiveness of different types of biochar in the remediation of heavy metal-contaminated soils, this study compares its results with several recent studies (Si et al., 2024; Sami et al., 2023; Guo et al., 2020). The comparison results (Table S6) indicate that the lignin-based biochar used in this study reduced Cd and Zn by 47.3 % and 85.5 %, respectively, during simulated aging, significantly outperforming the biochar used by Zhao et al. (2023). Importantly, the lignin-based biochar in this study not only exhibited superior efficiency in heavy metal removal but also significantly promoted plant growth and reduced plant uptake of heavy metals. This result is consistent with the observed improvement in plant growth using corn stalk biochar by Qianqian et al., (2022), where lettuce biomass and chlorophyll content in cadmium-contaminated soil increased by 74 %

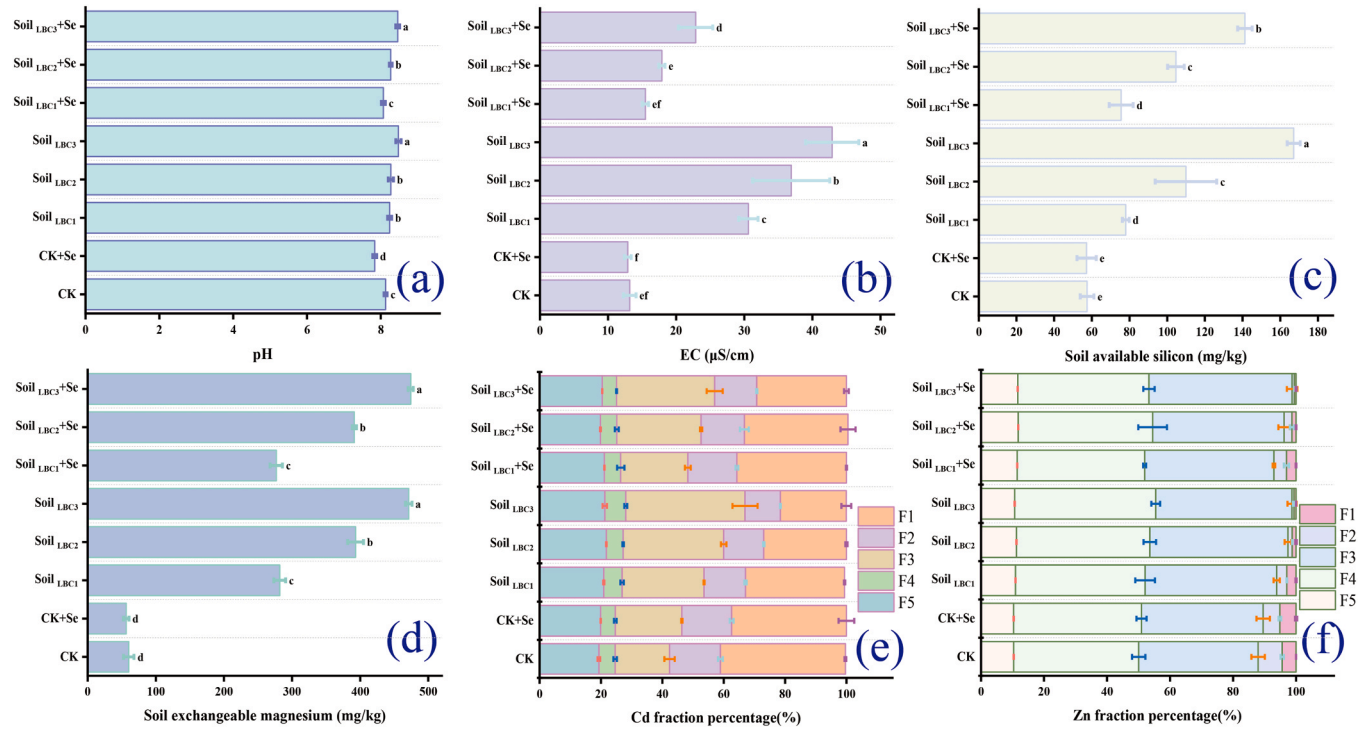

Fig. 5. Effect of application of aged LBC, foliar Se fertilizer and their combination on soil pH (a), DOC (b), A-Si (c), E-Mg (d), soil Cd (e) and Zn (f) forms. Different letters represent significant differences ($p \leq 0.05$) between treatments.

and 100 %, respectively. These comparisons highlight the critical importance of biochar type and aging treatment methods in enhancing the efficiency of heavy metal soil remediation and promoting plant growth.

3.4. Effects of aged LBC and Se on plant growth and photosynthesis

Heavy metal stress significantly impacted *pakchoi* growth under CK treatment. Cd and Zn exposure reduced transpiration rate (T_r), stomatal conductance (G_s), and photosynthesis rate (P_n) of *pakchoi* (Fig. 6). Additionally, chlorophyll content decreased markedly, likely due to chloroplast damage and disruption of photosynthetic pigment synthesis caused by heavy metal interference with light energy capture (Lagriffoul et al., 1998; Haider et al., 2024; Rizwan et al., 2017). In contrast, aged LBC and its combined treatment with Se significantly alleviated these effects. Simulated three–year aged LBC treatment increased T_r, G_s, and P_n by 53.17 %, 76.13 %, and 37.98 %, respectively. Notably, combined treatment of aged LBC and Se showed stronger effects, with T_r, G_s, and P_n increasing by 103.30 %, 120.72 %, and 81.40 %, respectively, demonstrating a synergistic effect. Aged LBC and aged LBC + Se treatments

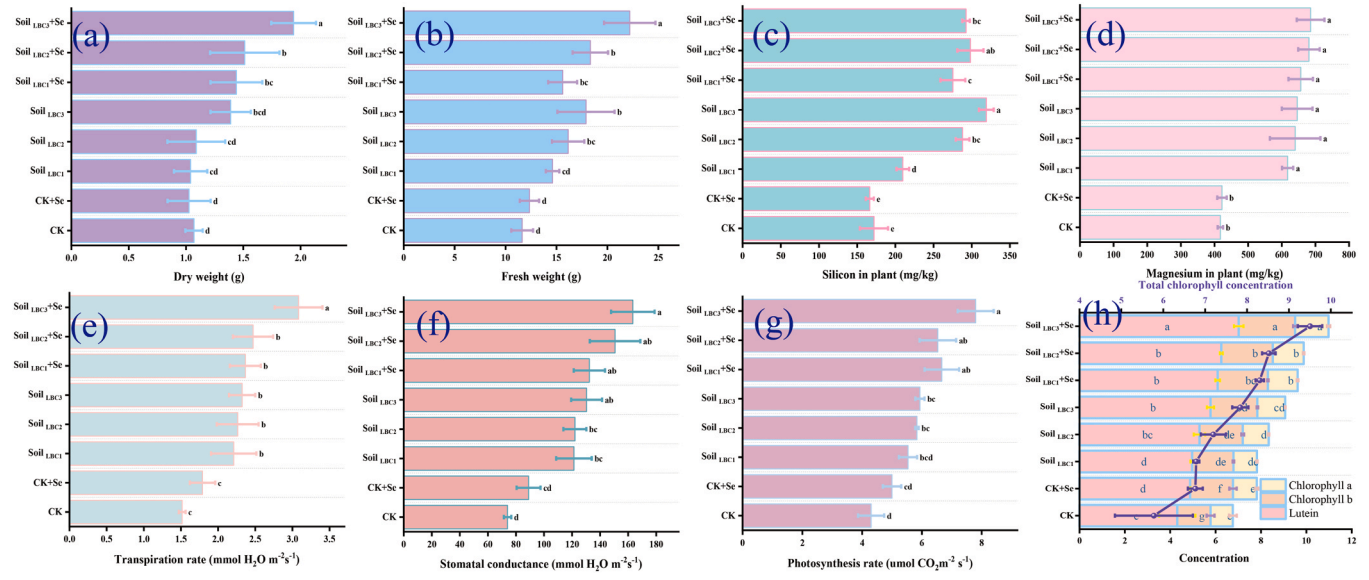

Fig. 6. Effect of application of aged LBC, foliar Se fertilizer and their combination on dry weight (a), fresh weight (b), content of silicon (c), magnesium (d), transpiration rate (e), stomatal conductance (f), photosynthetic rate (g), chlorophyll a, chlorophyll *b*, lutein, and total chlorophyll (h) in *pakchoi* under Cd and Zn stress.

significantly increased chlorophyll a, chlorophyll *b*, carotenoid, and total chlorophyll contents of *pakchoi*, with the latter showing notable increases of 62.90 %, 69.39 %, 49.86 %, and 64.55 %, respectively. This reveals the positive effect of nutrients released during LBC aging (such as Mg and Si) and Se addition on chlorophyll synthesis, enhancing photosynthesis efficiency. Further analysis indicated that aged LBC + Se treatment increased the fresh and dry weight of *pakchoi* by 90.88 % and 81.31 %, respectively, and enhanced the absorption of silicon and magnesium, with Si and Mg contents increasing by 21.97 %–85.56 % and 47.88 %–54.73 %, respectively. As a key element in chlorophyll synthesis and photosynthesis, Mg enhances photosynthetic efficiency, while Si promotes transpiration and improves water use efficiency by activating photosynthesis–related genes (Borbély et al., 2021; Hattori et al., 2005). After LBC aging, Mg and Si content in soil and plants increased, indicating that LBC, as a source of these elements, gradually releases them during aging, becoming an important source for *pakchoi* absorption. Moreover, LBC aging promotes the formation of nutrient–rich bacteria and changes the structure of rhizosphere bacterial communities, building a more favorable microbial ecosystem for plant growth, effectively alleviating heavy metal stress (Bandara et al., 2022). Se addition further strengthened this effect, promoting chlorophyll synthesis and increasing the rate of photosynthesis, achieving dual promotion of *pakchoi* growth. These enhancements can be attributed to reduced heavy metal bioavailability and the synergistic effects of silicon and magnesium released from aged biochar, which are essential for photosynthesis and plant metabolic processes. Figs. 7 and 8

3.5. Synergistic effects of aged LBC and Se

Under CK treatment, *pakchoi* exhibited significant oxidative stress induced by Cd and Zn, as evidenced by the lowest catalase (CAT) and superoxide dismutase (SOD) activities, indicating inhibition of the *pakchoi*'s antioxidant defense system and exacerbation of oxidative damage (Huang et al., 2021; Jiang et al., 2022). However, treatments with aged LBC and Se significantly enhanced CAT and SOD activities, indicating activation of the plant's antioxidant defense mechanisms. Specifically, the combined aged LBC + Se treatment showed more pronounced effects, increasing CAT and SOD activities by 73.07 %–137.20 % and 50.65 %–115.33 %, respectively, highlighting the synergistic advantage in enhancing antioxidant capacity.

Malondialdehyde (MDA) levels, a marker of oxidative stress and membrane damage, were significantly elevated under CK treatment. In contrast, aged LBC and Se treatments reduced MDA levels, with the combined LBC + Se treatment showing the most significant reduction (27.78 %–42.05 %), consistent with the increase in CAT and SOD activities. These findings confirm the effectiveness of these treatments in alleviating oxidative stress. Notably, while aged LBC treatment did not significantly alter reduced glutathione (GSH) content, the combination of aged LBC and Se increased GSH content by 22.16 %–33.23 %, further enhancing the plant's adaptability to heavy metal stress (Chakraborty and Mishra, 2020).

This study demonstrates that aged LBC + Se treatments alleviate oxidative damage in *pakchoi* under Cd and Zn stress by enhancing antioxidant enzyme activities and reducing oxidative stress markers. The beneficial effects may be attributed to the minerals (e.g., silicon) provided by LBC and the antioxidant properties of Se. The increase in silicon content during LBC aging may promote cell wall stability, limiting the translocation of heavy metals across cell membranes (Debona et al., 2017; He et al., 2013). Moreover, the adsorption properties of LBC help fix heavy metals near the cell wall, reducing their entry into the cytoplasm and organelles.

Se not only participates in antioxidant reactions but also may indirectly enhance plant antioxidant capacity by regulating the synthesis and metabolism of other antioxidants. The synergistic effect of aged LBC and Se appears to enhance *pakchoi*'s tolerance to heavy metal stress through multiple pathways, including the reduction of metal bioavailability and the improvement of antioxidant defense mechanisms. Further analysis of the subcellular distribution of Cd and Zn revealed

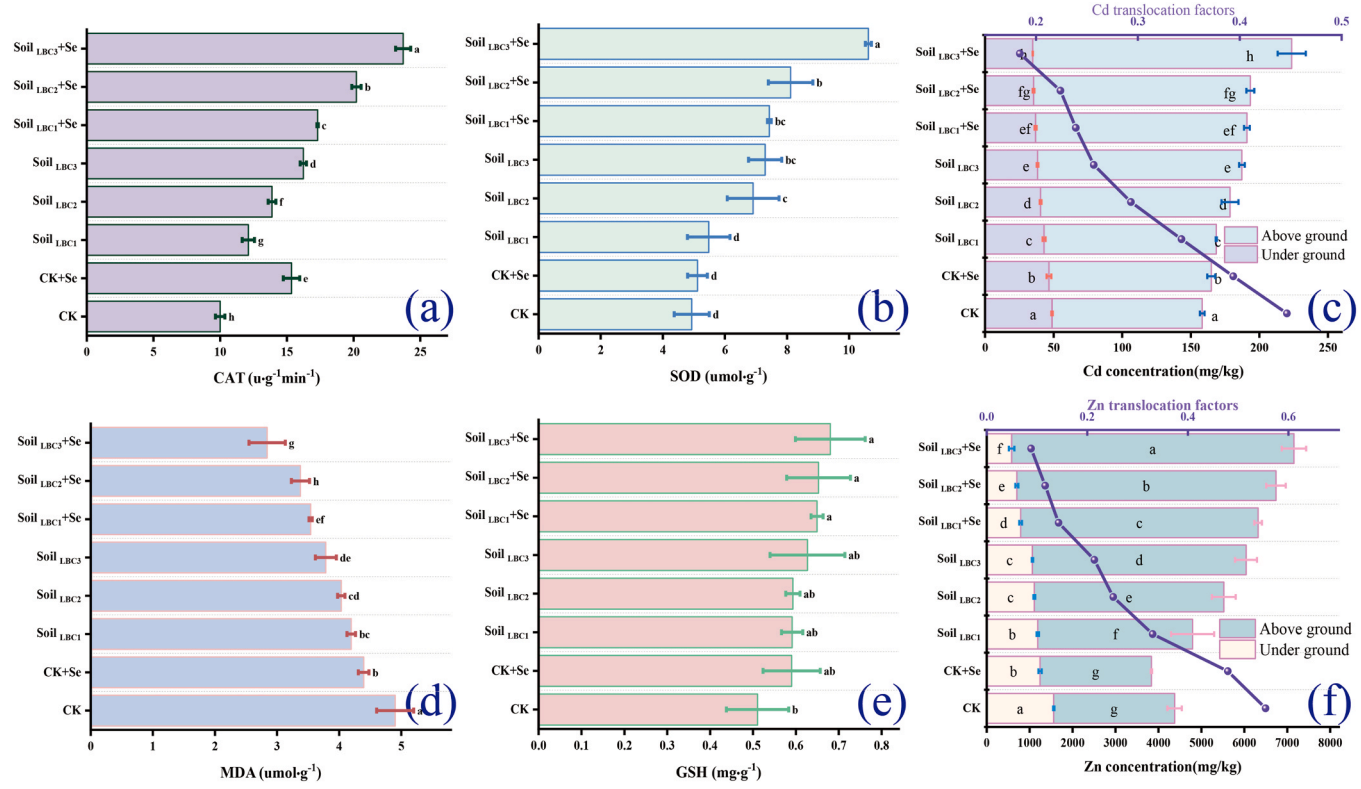

Fig. 7. Effect of application of aged LBC, foliar Se fertilizer and their combination on catalase (CAT) (a), superoxide dismutase (SOD) (b), malondialdehyde (MDA) (d), glutathione (GSH) (e), Cd (c), Zn (f) concentration in above ground, underground and translocation factor (TF) in *pakchoi* under Cd and Zn stress.

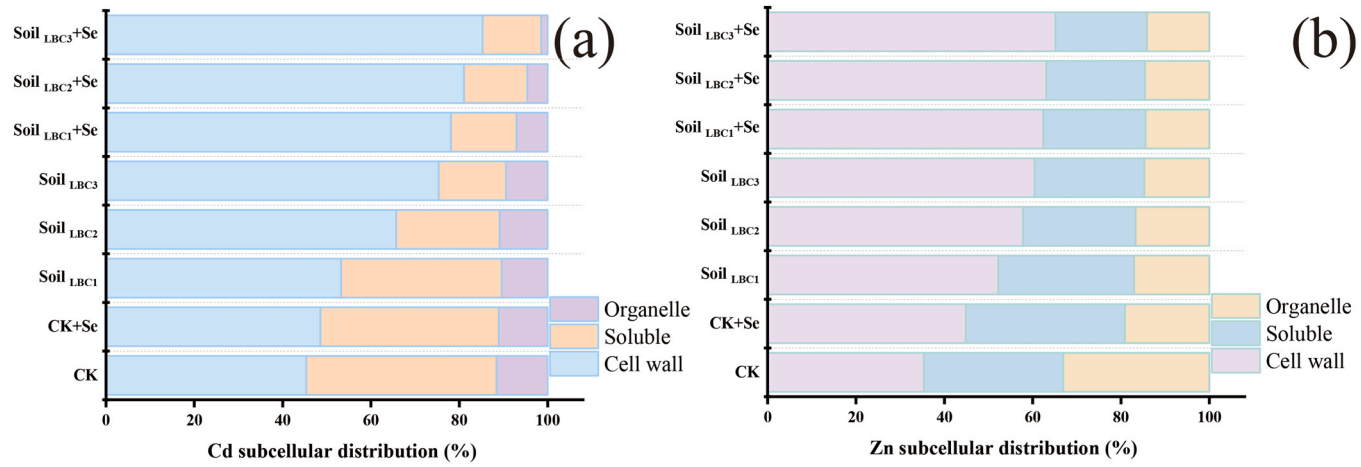

Fig. 8. Cd (a) and Zn (b) concentration of different subcellular fractions in *pakchoi* under Cd and Zn stress.

that LBC + Se treatment increased their accumulation in the cell wall, thereby enhancing its function as a barrier to heavy metals. This is in line with the detoxification strategy of plants, where the sequestration of heavy metals in the cell wall and vacuoles reduces their biotoxicity (Kollárová et al., 2019; Wei et al., 2021; Cui et al., 2023).

The synergistic interaction between biochar and selenium also improves photosynthesis efficiency and promotes plant growth. Sel enhances the activity of key antioxidant enzymes, which detoxify reactive oxygen species (ROS) produced during heavy metal stress (Chakraborty and Mishra, 2020; Jiang et al., 2022). When combined with biochar, selenium further amplifies this effect by promoting metal sequestration in plant cell walls, reducing the translocation of heavy metals into plant tissues (Wei et al., 2021; Cui et al., 2023). Additionally, biochar enhances the availability of essential nutrients like silicon and magnesium, which support plant metabolic processes and promote resilience to heavy metal toxicity (Hattori et al., 2005; Rizwan et al., 2017). These findings underscore the promising potential of the combined use of aged biochar and selenium in mitigating heavy metal contamination, while simultaneously promoting plant growth and resilience.

3.6. Future and limitations of aged ALB and Se treatments for sustainable agriculture

This study demonstrates the effectiveness of aged lignin-based biochar (LBC) and selenium (Se) treatments in reducing heavy metal bioavailability, improving soil health, and promoting plant growth, contributing to agricultural sustainability and food safety. However, the simulated aging process used in this study has limitations compared to natural field conditions. Factors such as microbial activity, seasonal environmental changes, and UV exposure may influence biochar aging in ways not captured in laboratory settings. Future studies should conduct field trials under varying environmental conditions and explore interactions with different soil types, such as acidic, alkaline, or sandy soils, to optimize biochar application strategies and ensure practical relevance. Despite these limitations, the simulated aging approach provides valuable insights into biochar's mechanisms and potential for sustainable soil management.

4. Conclusion

This study demonstrates the synergistic effects of aged lignin-based biochar (LBC) and foliar selenium (Se) application in mitigating soil heavy metal contamination and enhancing plant growth. Aged LBC improved soil properties, with available silicon and exchangeable magnesium increasing by 190.8 % and 730.4 %, respectively. These changes, along with enhanced functional groups (C-O, Si-O) and the formation of stable minerals ($Ca,MgCO_3$), increased LBC's ability to adsorb Cd and Zn, shifting the adsorption mechanism from Freundlich to Langmuir. The combined LBC + Se treatment increased *pakchoi*'s CAT and SOD activities by 137.20 % and 115.33 %, respectively, and reduced malondialdehyde (MDA) levels by 27.78 %–42.05 %, indicating reduced oxidative stress. Aged LBC retained Cd and Zn in the cell walls, minimizing their translocation to organelles and enhancing resistance to heavy metal stress. In conclusion, aged LBC effectively reduces heavy metal bioavailability, promotes plant growth, and activates antioxidant defenses. The synergistic effects of LBC and Se offer a promising strategy for improving soil health and mitigating heavy metal contamination in agriculture. Future research should explore the long-term impacts of LBC aging and Se application in field conditions.

Funding

The work was financially supported by the National Natural Science Foundation of China (31772390), Science and Technology Service Network Initiative Program (KFJ–STS–QYZD–177), and the Key Research and Development Plan of Ningxia Hui Autonomous Region (2023BEG02042).

CRediT authorship contribution statement

Diao She: Writing – review & editing, Supervision, Resources, Methodology, Funding acquisition. **Qing Zhen:** Writing – original draft, Formal analysis, Data curation. **Ruimei He:** Methodology. **Yongchao Yu:** Validation, Investigation, Formal analysis, Data curation. **Xianzhen Li:** Writing – original draft, Validation, Methodology, Investigation, Formal analysis, Data curation, Conceptualization.

Declaration of Competing Interest

The authors declare that they have no known competing financial interests or personal relationships that could have appeared to influence the work reported in this paper.

Appendix A. Supporting information

Supplementary data associated with this article can be found in the online version at doi:10.1016/j.indcrop.2025.120464.

Data availability

Data will be made available on request.

References

Aebi, H., 1984. Catalase in vitro. Elsevier, pp. 121–126. https://doi.org/10.1016/s0076–6879(84)05016–3.

Afzal, S., Alghanem, S.M.S., Alsudays, I.M., Malik, Z., Abbasi, G.H., Ali, A., Noreen, S., Ali, M., Irfan, M., Rizwan, M., 2024. Effect of biochar, zeolite, and bentonite on physiological and biochemical parameters and lead and zinc uptake by maize (Zea mays L.) plants grown in contaminated soil. J. Hazard. Mater. 469, 133927. https://doi.org/10.1016/j.jhazmat.2024.133927.

Arnon, D.I., 1949. Copper enzymes in isolated chloroplasts. Polyphenoloxidase in Beta vulgaris. Plant Physiol. 24 (1), 1–15. https://doi.org/10.1104/pp.24.1.1.

Bandara, T., Franks, A., Xu, J., Bolan, N., Wang, H., Tang, C., 2019. Chemical and biological immobilization mechanisms of potentially toxic elements in biochar–amended soils. Crit. Rev. Environ. Sci. Technol. 50 (9), 903–978. https://doi.org/10.1080/10643389.2019.1642832.

Bandara, T., Krohn, C., Jin, J., Chathurika, J.B.A.J., Franks, A., Xu, J., Potter, I.D., Tang, C., 2022. The effects of biochar aging on rhizosphere microbial communities in cadmium–contaminated acid soil. Chemosphere 303, 135–153. https://doi.org/10.1016/j.chemosphere.2022.135153.

Bolan, N., Hoang, S.A., Beiyuan, J., Gupta, S., Hou, D., Karakoti, A., Van Zwieten, L., 2021. Multifunctional applications of biochar beyond carbon storage. Int. Mater. Rev. 1–51. https://doi.org/10.1080/09506608.2021.1922047.

Bolan, S., Sharma, S., Mukherjee, S., Kumar, M., Rao, C.S., Nataraj, K.C., Bolan, N., 2023. Biochar modulating soil biological health: a review. Sci. Total Environ., 169585 https://doi.org/10.1016/j.scitotenv.2023.169585.

Borbély, P., Molnár, Á., Valyon, E., Ördög, A., Horváth–Boros, K., Csupor, D., Fehér, A., Kolbert, Z., 2021. The effect of foliar selenium (Se) treatment on growth, photosynthesis, and oxidative–nitrosative signalling of Stevia rebaudiana leaves. Antioxidants 10 (1), 72. https://doi.org/10.3390/antiox10010072.

Chakraborty, S., Mishra, A.K., 2020. Mitigation of zinc toxicity through differential strategies in two species of the cyanobacterium Anabaena isolated from zinc polluted paddy field. Environ. Pollut. 263, 114375. https://doi.org/10.1016/j.envpol.2020.114375.

Chen, X., Jiang, S., Wu, J., Yi, X., Dai, G., Shu, Y., 2024. Three–year field experiments revealed the immobilization effect of natural aging biochar on typical heavy metals (Pb, Cu, Cd). Sci. Total Environ. 912, 169–384. https://doi.org/10.1016/j.scitotenv.2023.169384.

Cui, T., Wang, Y., Niu, K., Dong, W., Zhang, R., Ma, H., 2023. Auxin alleviates cadmium toxicity by increasing vacuolar compartmentalization and decreasing long–distance translocation of cadmium in Poa pratensis. J. Plant Physiol. 282, 153919. https://doi.org/10.1016/j.jplph.2023.153919.

Debona, D., Rodrigues, F.A., Datnoff, L.E., 2017. Silicon's role in abiotic and biotic plant stresses. Annu. Rev. Phytopathol. 55 (1), 85–107. https://doi.org/10.1146/annurev–phyto–080516–035312.

Fridovich, I., 1975. Superoxide dismutases. Annu. Rev. Biochem. 44 (1), 147–159. https://doi.org/10.1146/annurev.bi.44.070175.001051.

Guo, X., Ji, Q., Rizwan, M., Li, H., Li, D., Chen, G., 2020. Effects of biochar and foliar application of selenium on the uptake and subcellular distribution of chromium in Ipomoea aquatica in chromium-polluted soils. Ecotoxicol. Environ. Saf. 206, 111184. https://doi.org/10.1016/j.ecoenv.2020.111184.

Haider, F.U., Ain, N.–, Khan, I., Farooq, M., Cai, L., Li, Y., 2024. Co–application of biochar and plant growth regulators improves maize growth and decreases Cd accumulation in cadmium–contaminated soil. J. Clean. Prod. 440, 140515. https://doi.org/10.1016/j.jclepro.2023.140515.

Hattori, T., Inanaga, S., Araki, H., An, P., Morita, S., Luxová, M., Lux, A., 2005. Application of silicon enhanced drought tolerance in Sorghum bicolor. Physiol. Plant. 123 (4), 459–466. https://doi.org/10.1111/j.1399–3054.2005.00481.x.

He, C., Wang, L., Liu, J., Liu, X., Li, X., Ma, J., Lin, Y., Xu, F., 2013. Evidence for 'silicon' within the cell walls of suspension-cultured rice cells. N. Phytol. 200 (3), 700–709. https://doi.org/10.1111/nph.12401.

Heath, R.L., Packer, L., 1968. Photoperoxidation in isolated chloroplasts. Arch. Biochem. Biophys. 125 (1), 189–198. https://doi.org/10.1016/0003–9861(68)90654–1.

Hou, R., Wang, L., O'Connor, D., Rinklebe, J., Hou, D., 2022. Natural field freeze–thaw process leads to different performances of soil amendments towards Cd immobilization and enrichment. Sci. Total Environ. 831, 154880. https://doi.org/10.1016/j.scitotenv.2022.154880.

Huang, H., Li, M., Rizwan, M., Dai, Z., Yuan, Y., Hossain, M.M., Cao, M., Xiong, S., Tu, S., 2021. Synergistic effect of silicon and selenium on the alleviation of cadmium toxicity in rice plants. J. Hazard. Mater. 401, 123393. https://doi.org/10.1016/j.jhazmat.2020.123393.

Jiang, S., Du, B., Wu, Q., Zhang, H., Deng, Y., Tang, X., Zhu, J., 2022. Selenium decreases the cadmium content in brown rice: foliar Se application to plants grown in Cd–contaminated soil. J. Soil Sci. Plant Nutr. 22 (1), 1033–1043. https://doi.org/10.1007/s42729-021-00711-w.

Khan, M.A., Ding, X., Khan, S., Brusseau, M.L., Khan, A., Nawab, J., 2018. The influence of various organic amendments on the bioavailability and plant uptake of cadmium present in mine–degraded soil. Sci. Total Environ. 636, 810–817. https://doi.org/10.1016/j.scitotenv.2018.04.299.

Kim, H.B., Kim, J.G., Alessi, D.S., Baek, K., 2024. Temporal changes in the mobility of As, Pb, Zn, and Cu due to differences in biochar stability caused by lignin content. Chem. Eng. J., 152567 https://doi.org/10.1016/j.cej.2024.152567.

Kollárová, K., Kusá, Z., Vatehová–Vivodová, Z., Lišková, D., 2019. The response of maize protoplasts to cadmium stress mitigated by silicon. Ecotoxicol. Environ. Saf. 170, 488–494. https://doi.org/10.1016/j.ecoenv.2018.12.016.

Krzyszczak, A., Dybowski, M.P., Zarzycki, R., Kobyłecki, R., Oleszczuk, P., Czech, B., 2022. Long–term physical and chemical aging of biochar affected the amount and bioavailability of PAHs and their derivatives. J. Hazard. Mater. 440, 129795. https://doi.org/10.1016/j.jhazmat.2022.129795.

Lagriffoul, A., Mocquot, B., Mench, M., Vangronsveld, J., 1998. Cadmium toxicity effects on growth, mineral and chlorophyll contents, and activities of stress related enzymes in young maize plants (Zea mays L.). Plant Soil 200, 241–250.

Lebrun, M., Palmeggiani, G., Renouard, S., Chafik, Y., Cagnon, B., Bourgerie, S., Morabito, D., 2023. Natural ageing of biochar improves its benefits to soil Pb immobilization and reduction in soil phytotoxicity. Environ. Geochem. Health 45 (8), 6109–6135. https://doi.org/10.1007/s10653–023–01617–5.

Lehmann, J., 2007. A handful of carbon. Nature 447 (7141), 143–144. https://doi.org/10.1038/447143a.

Li, X., Yu, Y., Zhang, Y., Wang, J., She, D., 2024b. Synergistic effects of modified biochar and selenium on reducing heavy metal uptake and improving *pakchoi* growth in Cd, Pb, Cu, and Zn–contaminated soil. J. Environ. Chem. Eng., 113170 https://doi.org/10.1016/j.jece.2024.113170.

Li, X., Zhang, Y., Huang, W., Luo, Y., Wang, J., She, D., 2024a. Silica–magnesium coupling in lignin–based biochar: a promising remediation for composite heavy metal pollution in environment. J. Environ. Manag. 363, 121392. https://doi.org/10.1016/j.jenvman.2024.121392.

Marcińczyk, M., Krasucka, P., Duan, W., Bo, P., Oleszczuk, P., 2024. Effect of chemical aging on phosphate adsorption and ecotoxicological properties of magnesium–modified biochar. Chemosphere 349, 140721. https://doi.org/10.1016/j.chemosphere.2023.140721.

Meng, Z., Huang, S., Lin, Z., Wu, J., 2022. First "unsaturated soils" view towards quantitative adsorption and immobilization mechanisms of Cd by biochar in soils during aging. Sci. Total Environ. 846, 157393. https://doi.org/10.1016/j.scitotenv.2022.157393.

Meng, Z., Huang, S., Zhao, Q., Xin, L., 2024. Respective evolution of soil and biochar on competitive adsorption mechanisms for Cd(II), Ni(II), and Cu(II) after 2–year natural ageing. J. Hazard. Mater. 469, 133938. https://doi.org/10.1016/j.jhazmat.2024.133938.

Menzembere, E.R.G.Y., Yinhai, H.E., Yingbo, D.O.N.G., Bing, L.I., Chenjing, L.I.U., Hai, L.I.N., Sambiani, L., 2023. Insight into modified biochars and their immobilizing effects on heavy metal (loid) s in contaminated soils: mechanisms and influencing factors. Pedosphere 33 (1), 23–33.

Mia, S., Dijkstra, F.A., Singh, B., 2018. Enhanced biological nitrogen fixation and competitive advantage of legumes in mixed pastures diminish with biochar aging. Plant Soil 424 (1–2), 639–651. https://doi.org/10.1007/s11104–018–3562–4.

Noctor, G., Foyer, C.H., 1998. Ascorbate and glutathione: keeping active oxygen under control. Annu. Rev. Plant Physiol. Plant Mol. Biol. 49 (1), 249–279. https://doi.org/10.1146/annurev.arplant.49.1.249.

Ouyang, X., Ma, J., Zhang, R., Li, P., Gao, M., Sun, C., Li, Y., 2022. Uptake of atmospherically deposited cadmium by leaves of vegetables: subcellular localization by NanoSIMS and potential risks (Doi.org/). J. Hazard. Mater. 431, 128624. https://doi.org/10.1016/j.jhazmat.2022.128624.

Qianqian, M., Haider, F.U., Farooq, M., Adeel, M., Shakoor, N., Jun, W., Cai, L., 2022. Selenium treated foliage and biochar treated soil for improved lettuce (Lactuca sativa L.) growth in Cd-polluted soil. J. Clean. Prod. 335, 130267. https://doi.org/10.1016/j.jclepro.2021.130267.

Rizwan, M., Ali, S., Hussain, A., Ali, Q., Shakoor, M.B., Zia–ur–Rehman, M., Farid, M., Asma, M., 2017. Effect of zinc–lysine on growth, yield and cadmium uptake in wheat (Triticum aestivum L.) and health risk assessment. Chemosphere 187, 35–42. https://doi.org/10.1016/j.chemosphere.2017.08.071.

Roberts, T.L., 2014. Cadmium and phosphorous fertilizers: the issues and the science. Procedia Eng. 83, 52–59. https://doi.org/10.1016/j.proeng.2014.09.012.

Sami, H., Ashraf, K., Sultan, K., Alamri, S., Abbas, M., Javied, S., uz Zaman, Q., 2023. Remediation potential of biochar and selenium for mitigating chromium-induced stress in spinach to minimize human health risk. South Afr. J. Bot. 163, 237–249. https://doi.org/10.1016/j.sajb.2023.10.049.

Shen, J., Huang, G., Yao, Y., Zhang, P., Rosendahl, S., 2024. Surface alteration on biochar in long–term application: insights into pyrolysis, freeze–thaw aging, and dissipation. Surf. Interfaces 46, 104118. https://doi.org/10.1016/j.surfin.2024.104118.

Si, T., Chen, X., Yuan, R., Pan, S., Wang, Y., Bian, R., Pan, G., 2024. Iron-modified biochars and their aging reduce soil cadmium mobility and inhibit rice cadmium uptake by promoting soil iron redox cycling. J. Environ. Manag. 370, 122848. https://doi.org/10.1016/j.jenvman.2024.122848.

Tóth, G., Hermann, T., Silva, M.R.D., Montanarella, L., 2016. Heavy metals in agricultural soils of the European Union with implications for food safety. Environ. Int. 88, 299–309. https://doi.org/10.1016/j.envint.2015.12.017.

Wei, W., Peng, H., Xie, Y., Wang, X., Huang, R., Chen, H., Ji, X., 2021. The role of silicon in cadmium alleviation by rice root cell wall retention and vacuole compartmentalization under different durations of Cd exposure. Ecotoxicol. Environ. Saf. 226, 112810. https://doi.org/10.1016/j.ecoenv.2021.112810.

Yuan, C., Gao, B., Peng, Y., Gao, X., Fan, B., Chen, Q., 2021. A meta-analysis of heavy metal bioavailability response to biochar aging: importance of soil and biochar properties. Sci. Total Environ. 756, 144058. https://doi.org/10.1016/j.scitotenv.2020.144058.

Zhao, X.Y., Zhang, Z.Y., Huang, Y.M., Feng, F.J., 2023. Enhancing the effect of biochar ageing on reducing cadmium accumulation in Medicago sativa L. Sci. Total Environ. 862, 160690. https://doi.org/10.1016/j.scitotenv.2022.160690.